2nd International Symposium on Magnetic Beaing
July 12-14, 1990, Tokyo, Japan

Experience with Magnetic Bearings Supporting a Pipeline Compressor

J. SCHMIED

Sulzer Escher Wyss Ltd., CH 8023 Zurich, Switzerland

Abstract

This paper describes theoretical and test results of the vibrational behaviour of a 6MW pipeline compressor supported on magnetic bearings, weighing about 1 ton and running at a maximum speed of 10000rpm. The theoretical model of the rotor bearing sytem, taking into account the bearing transfer function and the non collocation of sensor and actuator describes the behaviour very well in a frequency range up to 300Hz. The vibration level of the machine in operation is far below the limited capacity of magnetic bearings.

1. Introduction

The application of magnetic bearings described in this paper is in a pipeline compressor. A cross section of the machine is shown in fig.1.

The compressor is completely oilfree, assuring that the gas remains clean. This is achieved by the integrated design (the whole rotor is within the housing) and the magnetic bearings. Thanks to the integrated design no sealing against atmospheric pressure is necessary. Normally this is done by oil seals, which are a source of gas contamination. Bearing lubrication has to be avoided, because the bearings are within the housing surrounded by the gas. The compressor is driven by an induction motor of variable speed, which is in the middle of the shaft and which is cooled by the compressed gas.

The rated power of the motor is 6MW. The maximum speed is 10000rpm. The whole rotor weighs 1 ton. According to the S2M reference list of January 90 for heavy turbomachinery applications of magnetic bearings (fig.2) it is presently the heaviest rotor running at a speed of 10000rpm.

In the course of the development of this machine a variety of theoretical

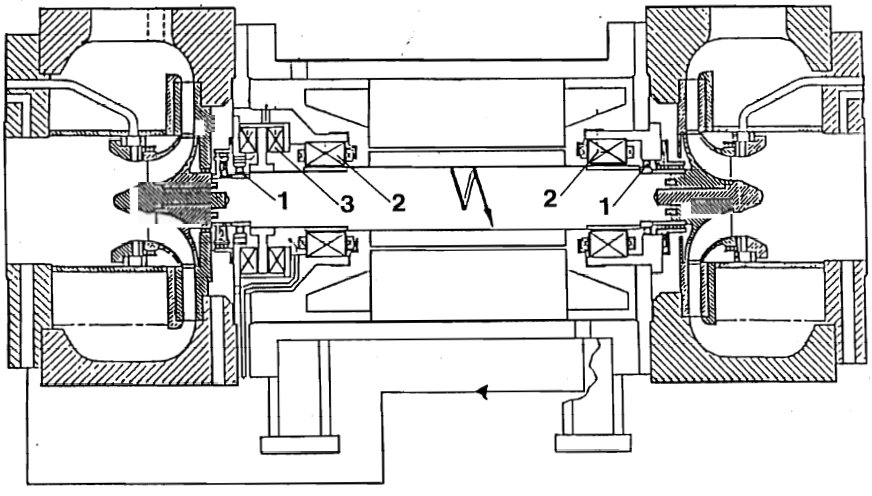

1 auxiliary bearing
2 radial magnetic bearing
3 thrust magnetic bearing

Fig.1
Cross section of the compressor

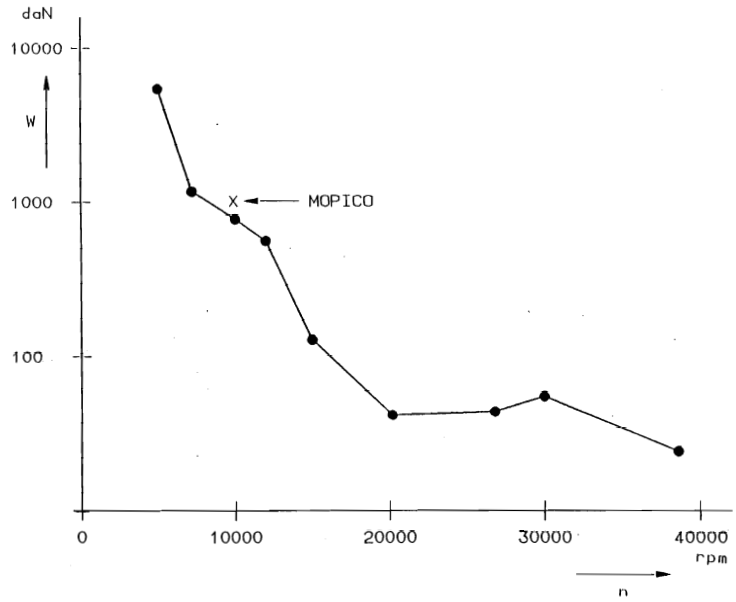

Fig.2
Extreme speeds and weights of large turbomachines supported on magnetic bearings (S2M reference list)

investigations were carried out. The theoretical models of the rotor and the magnetic bearings are described. Theoretical results are reported as well as test results.

2. Modeling the Rotor Bearing System

2.1 The Rotor

Fig.3 shows the finite element model of the rotor. It has 21 elastic shaft elements and three rigid disks. Each node has four coordinates, two for the displacements in direction of the horizontal and vertical axis and two for the rotations around these axis. Hence the model has 88 degrees of freedom. The elements take into account stiffness and all inertia effects (including gyroscopic effects), whereas the disks only have inertia properties.

Table 1 shows the diameter of each element and the additional mass per length modeling the sleeves and laminations shrunk on the rotor. In the region of the motor (element 12 to 15) the given diameter only determines the stiffness, and the added mass per length is the total rotor mass per length.

2.2 The Magnetic Bearing

Fig.4 shows the elements of a magnetic bearing. It consists of a sensor, controller, amplifier and actuator for each direction. The bearing characteristic is basically determined by the controller. Fig.5 shows a block diagram of the analog controller. The filters in the first two blocks condition the measured displacement signal x_m. The phase lead cells produce a damping effect and the integrator prevents a large static deflection. A model of

MB magnetic bearing
AB auxiliary bearing
IP impeller
TB thrust disk

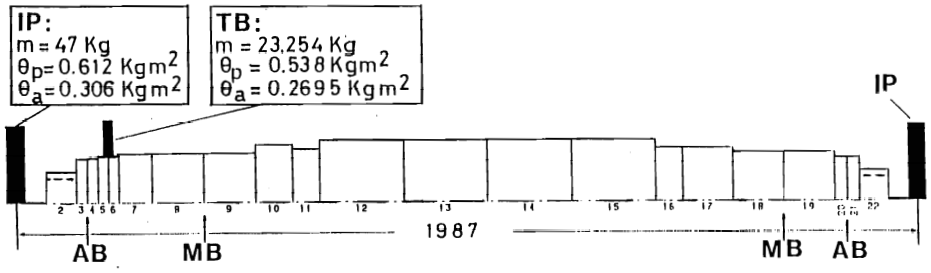

Fig.3
Finite element model of the rotor

Table 1 : Element diameters and added mass per length of the shaft elements

element number	outer diam. [mm]	added mass [kg/m]
2	130.0[1)]	190.0
3/4/20/21	167.6	49.39
5/6	178.0	
7	184.0	73.61
8/9/18/19	186.0	72.20
10	215.0	
11/16	200.0	386.04
12÷15	218.0	735.22[2)]
17	200.0	069.25
22	130.0[1)]	097.46

1) hollow shaft, inner diameter 112.0 mm
2) total mass of the elements 12÷15

the bearing is created by modeling the controller according to fig.5. The sensor, the amplifier and actuator are taken into account by the constant scaling factor SF. In reality the transfer functions of these elements are not a constant. The amplifier plus actuator has a perceptible amplitude and phase loss with

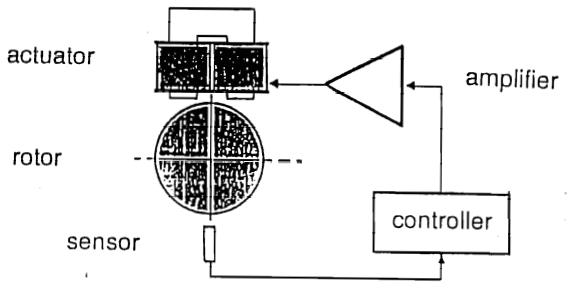

Fig.4 Elements of a magnetic bearing

increasing frequency. At 1000Hz the amplitude and phase lag are about 1% and 30 degree respectively. This effect is neglected as its influence is very small at lower frequencies. Fig.6 shows the open loop transfer function between the bearing force and the measured displacement of the thus modeled bearing.

The bearing only creates damping if the phase angle of the transfer function is between 0 and +90 degrees, which in this case is only for frequencies above 20Hz. This is due to the integral part in the controller. All natural frequencies of the rotor bearing system therefore must be above 20Hz to prevent instability.

The damping and stiffness coefficient of the magnetic bearing can be calculated by

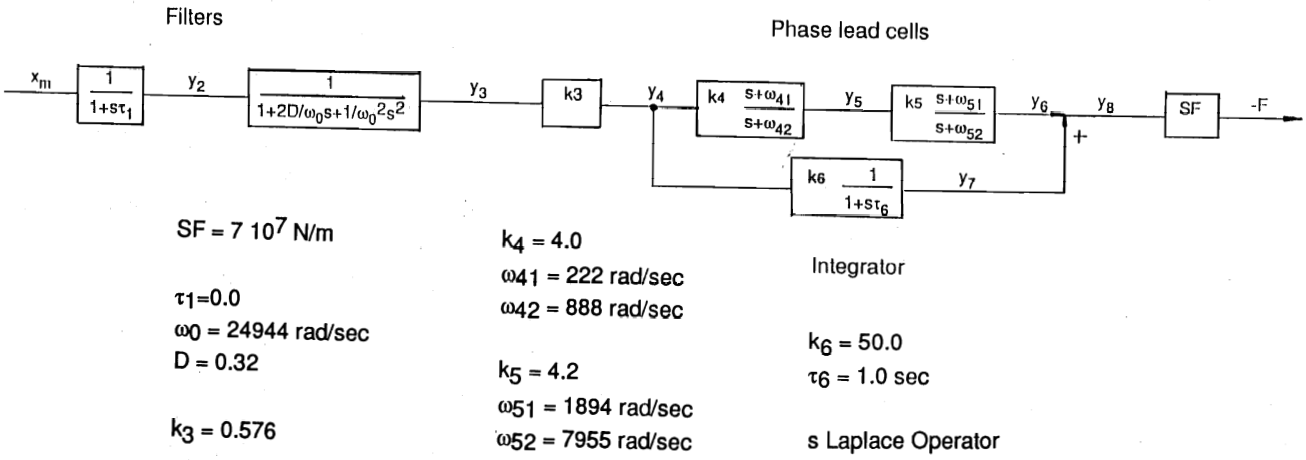

Fig.5 Block diagram of the controller
(with courtesy of Magnetic Bearing Inc.)

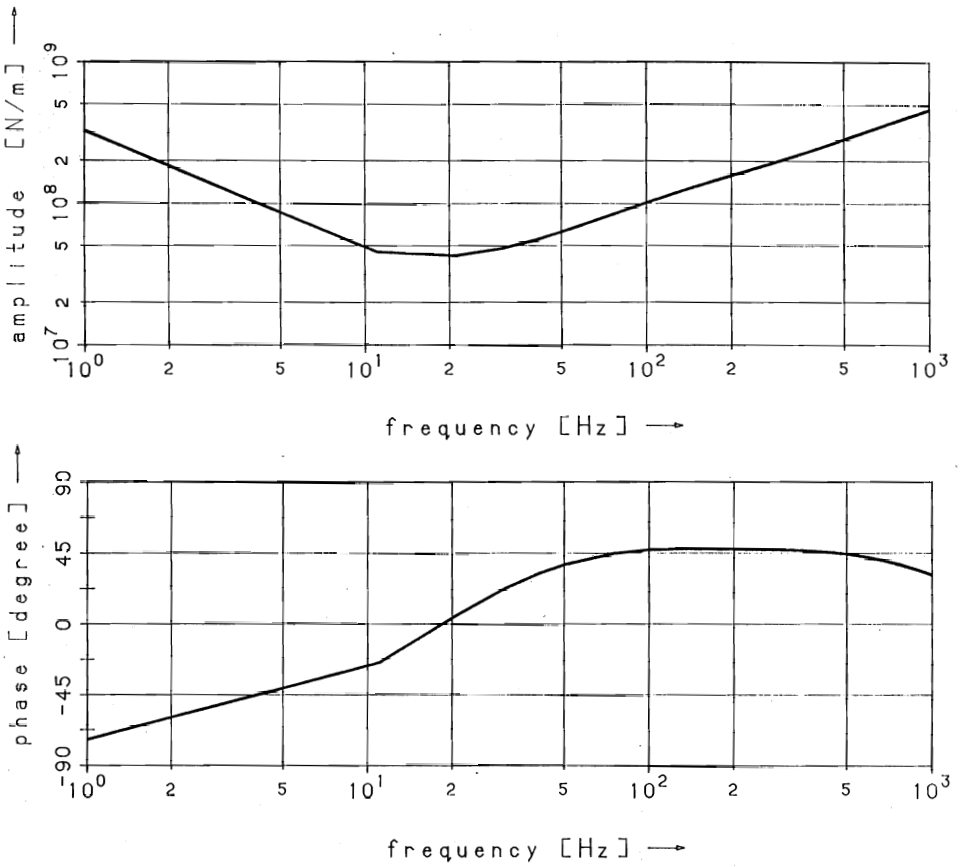

Fig.6
Open loop transfer function of the bearing

taking the real part of the transfer function as the stiffness and the imaginary part divided by the angular frequency as the damping coefficient. Fig.7 shows the thus calculated coefficients as a function of the frequency compared to those of a four tilting pad oil bearing suitable for this rotor. The oil bearing coefficients do not depend on the frequency but on the rotating speed. The shown coefficients are for a speed of 10000rpm. It can be seen that in the frequency range of 30 to 200Hz the magnetic bearing has approximately the same damping coefficient and a stiffness coefficient which is about one third to one sixth.

In the appendix is described how the magnetic bearing is integrated into the finite element model of the rotor. The rotor bearing model thus created also takes into account the slightly different axial position (non collocation) of the sensor and the actuator. The model allows a stability analysis (i.e. to calculate damping factors) of the combined rotor bearing system as well as response calculations to be carried out.

A linear model as described above however is only correct for limited rotor displacements, since the actual bearing force is a nonlinear function of the rotor displacement and velocity /1,2/. The nonlinearities limit the performance of magnetic bearings. Two very important limits are the peak force capacity of the bearing, which is determined by the magnetic saturation and the maximum slew rate, which is limited by the maximum output voltage of the amplifier. Fig.8 shows the maximum amplitude of a harmonic bearing force as a function of the frequency. At lower frequencies the limit is due to the magnetic saturation and at higher frequencies due to the amplifier saturation.

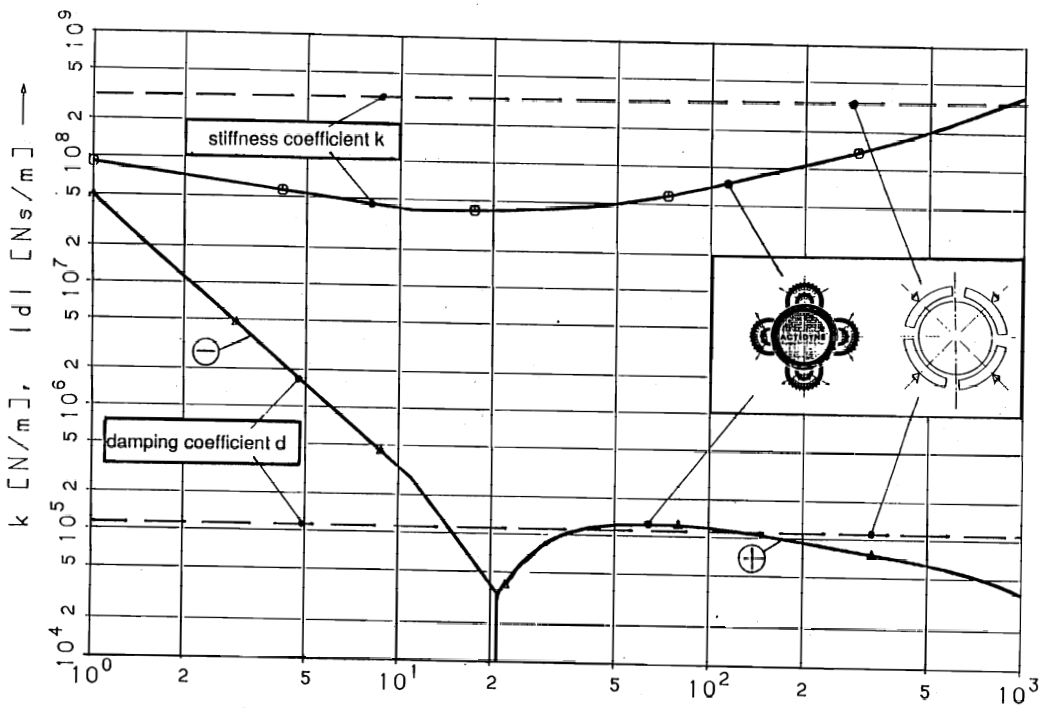

Fig.7 Siffness and damping coefficient of the magnetic bearing and an oil bearing

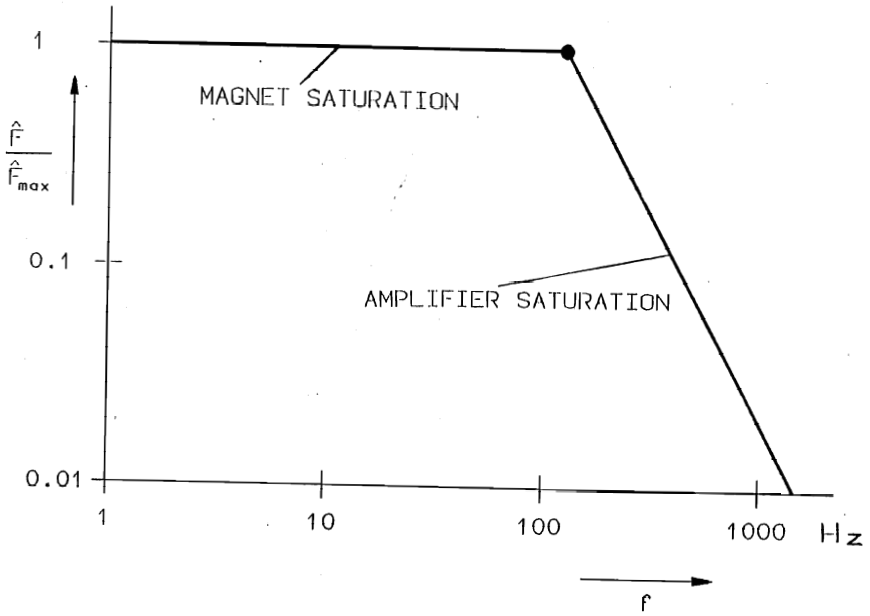

Fig.8
Limits of a harmonic bearing force
F_{max} = 10000N

3. Theoretical and Test Results

All the analyses in this section were carried out by means of the finite element rotor dynamic program MADYN /3/.

Fig. 9 shows calculated damping factors and frequencies of the first three forward whirling modes of the rotor at a speed of 10000rpm. For comparison the diagram also shows results for the rotor supported on the oil bearings with the damping and stiffness coefficients of fig.7 . It can be seen that the first two modes, which are below the maximum operating speed have a lower frequency but a much better damping for a rotor supported on magnetic bearings. This is achieved with a damping coefficient, which is approximately the same as for oil bearings, and a stiffness coefficient, which is much lower.

The theoretical rotor model results as described above are very well confirmed in a frequency range up to 300Hz by comparison of calculated and measured closed loop transfer functions. Fig.10 shows the calculated transfer function for an excitation by means of the magnetic actuators on both sides and a displacement measurement with the bearing sensors. The phase angle of 90 degrees at the frequency 0 is due to the integrator in the controller. The phase angle of -90 degrees at about 45Hz indicates the first mode. A peak in the amplitude is not very clear because of the good damping and the logarithmic scale. A phase shift or peak due to the second mode is not visible, because it is not excited, since the excitation is on both sides. The phase shifts between 130 and 150Hz are due to the changing shape (transition from the first rigid body mode to the first bending mode). The phase angle of -90 degrees and the amplitude peak at about 180Hz indicate the third mode, which is the first bending mode. The frequency is not as high as in fig.9 because the rotating speed here is only 4000rpm instead of 10000rpm in fig.9, hence the gyroscopic effect is less.

The model does not describe the real rotor with a sufficient accuracy at frequencies above 300Hz. Considering the simplifications in the rotor and bearing model (section 2), this is not surprising. The natural frequencies of the fourth and fifth mode (at 380Hz and 640Hz) do still coincide quite well (the maximum deviation is about 5%), but the stability is not predicted well. The fourth and fifth mode in practice became unstable before the controller was properly tuned. The theoretical model did not predict these instabilities. According to the theoretical results the fourth mode has on one side a node between sensor and actuator, hence one

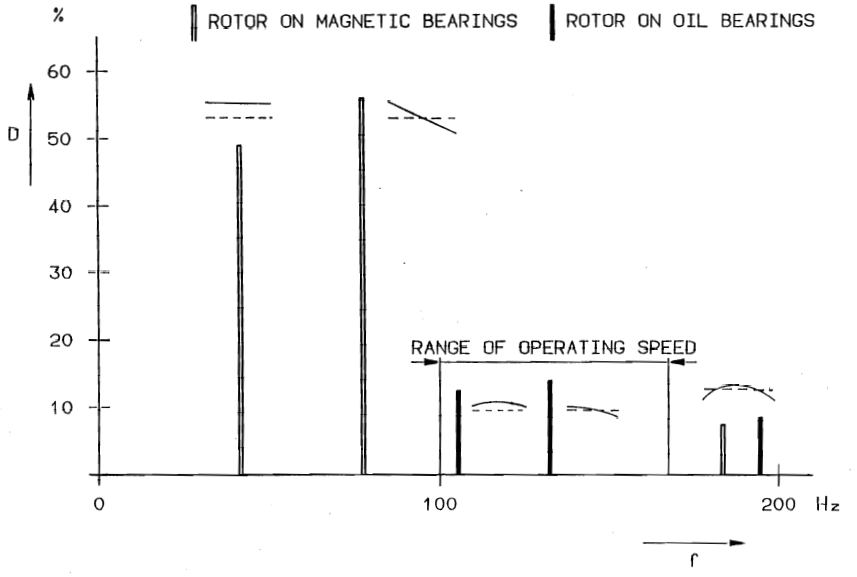

Fig.9
Damping factors and frequencies of the first three forward whirling modes of the rotor in oil and magnetic bearings

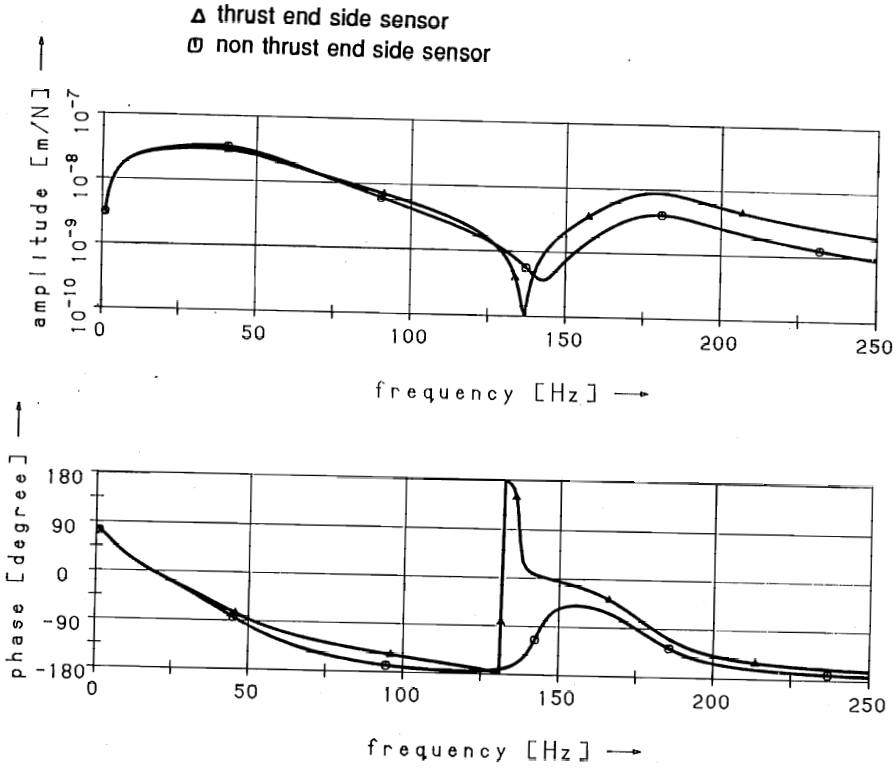

Fig.10
Closed loop transfer function, excitation with the actuators of both bearings, response at the sensors

bearing tends to excite rather than damp the system (also see /4/), but the other bearing still provides enough damping to prevent an instability (the calculated damping factor has the very low value of 0.7%). In practice both mentioned modes had to be stabilized by a notch filter at the natural frequencies of the two modes.

The theoretical model is only unstable at frequencies above 1500Hz due to the non collocation of sensor and actuator and also due to negative phase angles (=negative damping) of the open loop bearing transfer function (not shown in fig.6). At these frequencies however the model is in any case too inaccurate. In practice instabilities at higher frequencies than the fifth mode did not occur. These modes seem to be sufficiently damped by the internal damping to compensate any excitation from the bearing.

Fig.11 shows the measured once per revolution bearing force amplitudes for a run up to 10000rpm with full load in relation to the limits of the bearing mentioned in section 2. It can be seen that at full speed the level is still only 50% of the limit. This is the level for a very fast run up of the cold rotor within 2 minutes, when the rotor is not yet fully thermally balanced. After about 15 minutes, when the rotor is warm, or for a slower run up within 15 minutes, the level is only about half of that shown on fig.11.

Acknowledgements

I want to thank my colleagues from ACEC, the motor manufacturer, and from Magnetic Bearing Inc. for the good cooperation throughout this joint project.

References

/1/ Maslen, E., et al.: Practical Limits to the Performance of Magnetic Bearings: Peak Force, Slew Rate and Displacement Sensitivity. ASME Journal of Tribology, Vol. 111, April 1989.

/2/ Traxler, A.: Eigenschaften und Auslegung von berührungsfreien elektromagnetischen Lagern. Dissertation ETH Zürich 1985.

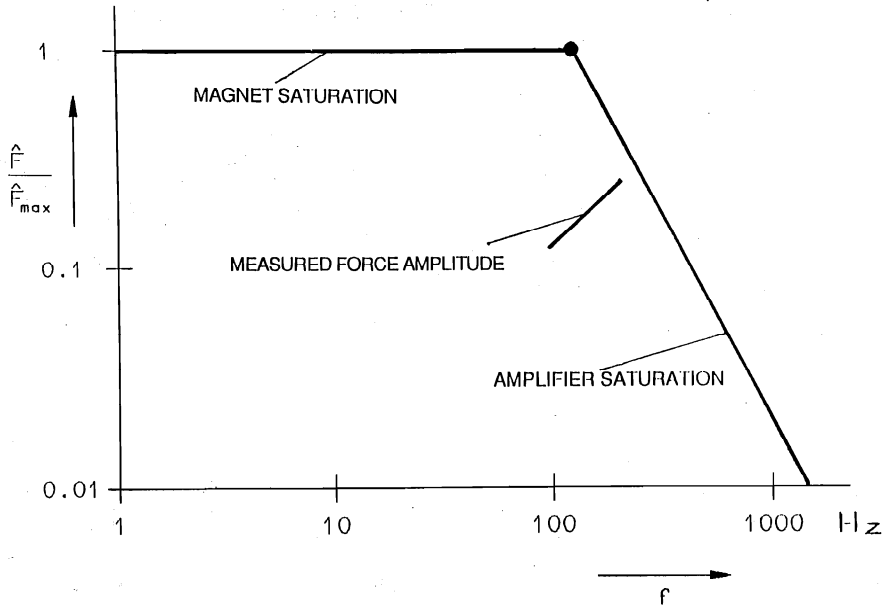

Fig.11
Measured once per revolution force amplitude versus bearing limits

/ 3 / Klement, H.D., Schilling, W.: Schwingungsberechnungen mit dem Programmsystem MADYN. VDI Berichte 786, 1989.

/ 4 / Salm, J., Schweitzer, G.: Modeling and control of a flexible rotor with magnetic bearings. Paper C277/84, Institution of Mechanical Engineers, 1984.

Appendix: Integrating the Magnetic Bearing into the Finite Element Model of the Rotor

For this purpose the finite element rotor model is expanded to include the "controller coordinates" y_2 to y_8 (see fig.5) for each bearing and direction. The coordinate x_m in fig.5 is the translatory coordinate of the finite element model of the rotor at the measuring position in the direction of the sensor. The bearing force F is applied at a node in the middle of the magnetic bearing in the direction of the actuator. The corresponding coordinate is x_F. The direction of the sensor and the actuator coincide, their axial position however does not. The block diagram (fig.5) corresponds to the following equations in the time domain:

$$\tau_1 \dot{y}_2 + y_2 = x_m \qquad \text{(A1)}$$

$$\ddot{y}_3 + 2D\omega_0 \dot{y}_3 + \omega_0^2 y_3 = \omega_0^2 y_2 \qquad \text{(A2)}$$

$$y_4 = k_4 y_3 \qquad \text{(A3)}$$

$$\dot{y}_5 + \omega_{42} y_5 = k_4 (y_4 + \omega_{41} y_4) \qquad \text{(A4)}$$

$$\dot{y}_6 + \omega_{52} y_6 = k_5 (y_5 + \omega_{51} y_5) \qquad \text{(A5)}$$

$$\tau_6 \dot{y}_7 + y_7 = k_6 y_4 \qquad \text{(A6)}$$

$$y_8 = y_6 + y_7 \qquad \text{(A7)}$$

$$-F = SF\, y_8 \qquad \text{(A8)}$$

The coefficients of x_m and the "controller coordinates" $y_{2\text{-}8}$, as well as the coefficients of their first and second derivatives have to be introduced into the appropriate lines and columns of the stiffness, damping and mass matrices of the expanded finite element model, as is shown below. When using the finite element program MADYN /3/ this can be achieved by general matrix addition.

Lines and columns of the expanded mass matrix concerned by the bearing:

	x_m	y_2	y_3	y_4	y_5	y_6	y_7	y_8	x_F
x_m									
y_2									
y_3			1						
y_4									
y_5									
y_6									
y_7									
y_8									
x_F									

Lines and columns of the expanded damping matrix concerned by the bearing:

	x_m	y_2	y_3	y_4	y_5	y_6	y_7	y_8	x_F
x_m									
y_2		τ_1							
y_3			$2D\omega_0$						
y_4									
y_5				$-k_4$	1				
y_6					$-k_5$	1			
y_7							τ_6		
y_8									
x_F									

Lines and columns of the expanded stiffness matrix concerned by the bearing

	x_m	y_2	y_3	y_4	y_5	y_6	y_7	y_8	x_F
x_m									
y_2	-1	1							
y_3		$-\omega_0^2$	ω_0^2						
y_4			$-k_3$	1					
y_5				$-k_4\omega_{41}$	ω_{42}				
y_6					$-k_5\omega_{51}$	ω_{52}			
y_7				$-k_6$			1		
y_8						-1	-1	1	
x_F								SF	